· Article ·
doi: 10.13679/j.advps.2015.3.00249

Advances in Polar Science
September 2015 Vol. 26 No. 3: 249-255

Variation characteristics of carbon monoxide and ozone over the course of the 2014 Chinese National Arctic Research Expedition

LI Bokun[1], BIAN Lingen[2]*, ZHENG Xiangdong[2], DING Minghu[2] & XIE Zhouqing[1]*

[1] Institute of Polar Environment, University of Science and Technology of China, Hefei 230026, China;
[2] Chinese Academy of Meteorological Sciences, Beijing 100081, China

Received 24 June 2015; accepted 11 September 2015

Abstract The concentrations of carbon monoxide and ozone in the marine boundary layer were measured during the 6th Chinese National Arctic Research Expedition (from July to September, 2014). Carbon monoxide concentration ranged between 47.00 and 528.52 ppbv with an average of 103.59 ± 40.37 ppbv. A slight decrease with increasing latitude was observed, except for the extremely high values over the East China Sea which may be attributed to anthropogenic emissions. Ozone concentration ranged between 3.27 and 77.82 ppbv with an average of 29.46±10.48 ppbv. Ozone concentration decreased sharply with increasing latitude outside the Arctic Ocean (during both the northward and the southward course), while no significant variation was observed over the Arctic Ocean. The positive correlation between carbon monoxide and ozone in most sections suggests that the ozone in the marine boundary layer mainly originated from photochemical reactions involving carbon monoxide.

Keywords **carbon monoxide, ozone, marine boundary layer, temporal and spatial variation**

Citation: Li B K, Bian L G, Zheng X D, et al. Variation characteristics of carbon monoxide and ozone over the course of the 2014 Chinese National Arctic Research Expedition. Adv Polar Sci, 2015, 26: 249-255, doi: 10.13679/j.advps.2015.3.00249

1 Introduction

Carbon monoxide is a major pollutant in the atmosphere. Over-exposure to carbon monoxide can directly cause adverse health effects. It is also one of the indirect greenhouse gases in the atmosphere[1]. The carbon monoxide in the atmosphere originates via emissions arising from the combustion of fossil fuels and biomasses as well as the photochemical transformation of certain hydrocarbons (e.g. methane)[2-3]. The removal of carbon monoxide from the atmosphere relies on a reaction with a hydroxyl radical (OH)[4]. Thus, by changing the concentration of hydroxyl radicals in the troposphere, natural or anthropogenic disturbances of tropospheric carbon monoxide can influence the chemical properties of the troposphere[5-6]. The lifespan of tropospheric carbon monoxide varies with latitude and season, ranging from several weeks to over one year. The lifespan is mostly determined by the tropospheric hydroxyl radical concentration[7-9].

Ozone is also one of the pollutants in the troposphere as well as a major greenhouse gas[10-12]. The tropospheric ozone derives from both natural inputs via the stratosphere and photochemical processes involving hydrocarbons and nitrogen oxides (NO*x*) in the troposphere[13]. The nitrogen oxides and volatile organic matters from vehicle exhaust and industrial emission are the main precursors of ozone generated from chemical reactions in the troposphere[14]. Because of the

* Corresponding authors (email: blg@cams.cam.gov.cn (B.L.G.) , zqxie@ustc.edu.cn (Z.Q.X.))

high oxidizability of ozone, it is closely connected with many chemical processes, especially photochemical reactions with greenhouse gases[15-16].

Continuous measurements of the concentrations of carbon monoxide and ozone in the marine boundary layer were carried out aboard the R/V *XUE LONG* icebreaker. The measurements may provide the latest data on the spatial variations of carbon monoxide and ozone in the marine boundary layer from mid-latitude seas to the northern high-latitude sea including the Arctic Ocean. Moreover, these data can aid in the understanding of the relationship between changes of the tropospheric ozone in the Arctic region and the climate change at mid- and high-latitudes[17].

2 Experimental methods

2.1 The expedition

The R/V *XUE LONG* icebreaker, the R/V of the 6th Chinese National Arctic Research Expedition, departed from Shanghai harbor on July 11th 2014 and returned on September 22nd 2014. Various scientific investigations were carried out during the expedition. The course of the journey is shown in Figure 1. The cruise path covered the East China Sea, the Sea of Japan, the Sea of Okhotsk, the Bering Sea, the Chukchi Sea, the Beaufort Sea, and the Arctic Ocean.

2.2 In-situ measurements

The carbon monoxide measurements were performed using an internet-enabled automatic infrared carbon monoxide analyzer (model EC9830T, Ecotech Inc., Australia). The ozone measurements were performed using an internet-enabled automatic ozone analyzer (model EC9810B, Ecotech Inc., Australia). The analyzers had been calibrated before departure based on the NIST standard system.

2.3 Air mass back trajectory

Air mass back trajectory was performed according to the transmission diffusion model of HYSPLIT (Hybrid Single-Particle Lagrangian Integrated Trajectory) developed by the Air Resources Laboratory of the United States National Oceanic and Atmospheric Administration. These calculations were carried out to identify the source of the air masses[18-19].

3 Results and discussion

As the analyzers were installed at the bow of R/V *XUE LONG* icebreaker and the engine of R/V *XUE LONG* icebreaker was at the stern, the measurements were not affected by the icebreaker's emission on most occasions. However the data collected when wind was coming from the stern were removed in order to eliminate the pollution coming from the stack.

3.1 The temporal and spatial variations of carbon monoxide

Carbon monoxide concentration measured during the 6th Chinese National Arctic Research Expedition ranged between 47.00 and 528.52 ppbv with an average of 103.59 ± 40.37 ppbv. The time series is shown in Figure 2.

The whole cruise is divided into six sections, and the average, maximum, and minimum carbon monoxide concentration of each section is shown in Table 1.

As shown in Table 1, the concentrations of carbon monoxide were high over the East China Sea and the Sea of Japan. The maximum (528.52 ppbv) of the expedition was observed on the northward course over the East China Sea; for the southward leg of the journey, the maximum (220.12 ppbv) was also observed over the East China Sea. Besides the East China Sea and the Sea of Japan, observations of carbon monoxide concentrations in the other sections, such as the Sea of Okhotsk, the Bering Sea, and the Arctic Ocean, were at a relatively low level. The minimum (47.00 ppbv) was observed over the Arctic Ocean.

The concentration of carbon monoxide in the atmosphere is greatly affected by human activities. Consequently, the concentrations were much higher over the East China Sea and the Sea of Japan than other sections, such as the Sea of Okhotsk, the Bering Sea, and the Arctic Ocean. After R/V *XUE LONG* icebreaker left the Sea of Japan for the high-latitude seas, the concentrations sharply decreased to very low levels and were relatively stable (Figure 3).

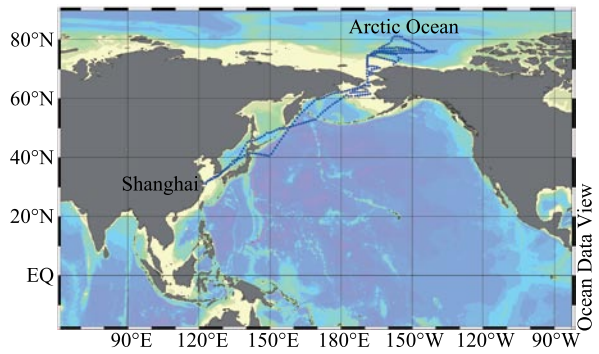

Figure 1 Track of the R/V *XUE LONG* icebreaker cruise during the 6th Chinese National Arctic Research Expedition.

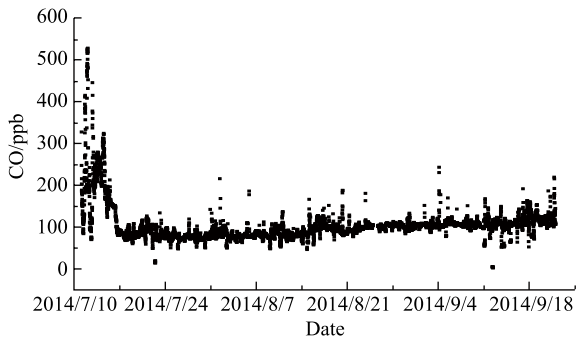

Figure 2 The time series of the concentration of carbon monoxide during the cruise.

Table 1 Carbon monoxide concentration in different sections

Sections	Date	Average/ppbv	Maximum/ppbv	Minimum/ppbv	Sample number
	7-11~7-13	215.01	528.52	70.64	260
East China Sea	9-20~9-22	124.41	220.12	100.92	140
	Overall	183.30	528.52	70.64	400
	7-13~7-15	218.63	324.93	123.84	366
Sea of Japan	9-18~9-20	116.88	154.37	72.08	324
	Overall	170.85	324.93	72.08	690
	7-15~7-19	99.51	167.15	60.96	549
Sea of Okhotsk	9-14~9-118	111.48	192.35	53.37	664
	Overall	106.07	192.35	53.37	1213
	7-19~7-28	82.71	134.63	48.48	1230
Bering Sea	9-9~9-14	105.49	168.79	52.88	582
	Overall	89.86	168.79	48.48	1755
Arctic Ocean	7-28~9-9	94.35	243.65	47.00	5988
Overall	7-11~9-22	103.59	528.52	47.00	10047

In order to investigate the potential influence due to the air mass, 7-day back trajectories of the respective carbon monoxide maximum observed over the northward and the southward legs of the journey were performed using the HYSPLIT model (Figure 4). As shown in Figure 4, the back trajectories imply that the air masses passed through Northeast Asia. These regions have intensive industrial activities. Industrial and vehicle exhaust emissions may have contributed greatly to the maximum observed over both the northward and the southward courses. For comparison, another back trajectory was performed (Figure 5), where the minimum was observed. The result indicates that the air mass mainly passed through the Arctic Ocean and the Northwest

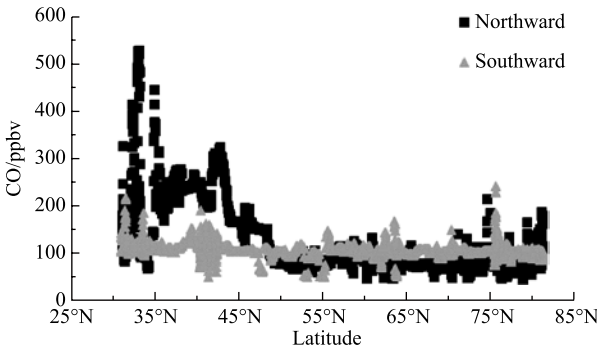

Figure 3 The concentration of carbon monoxide at different latitudes.

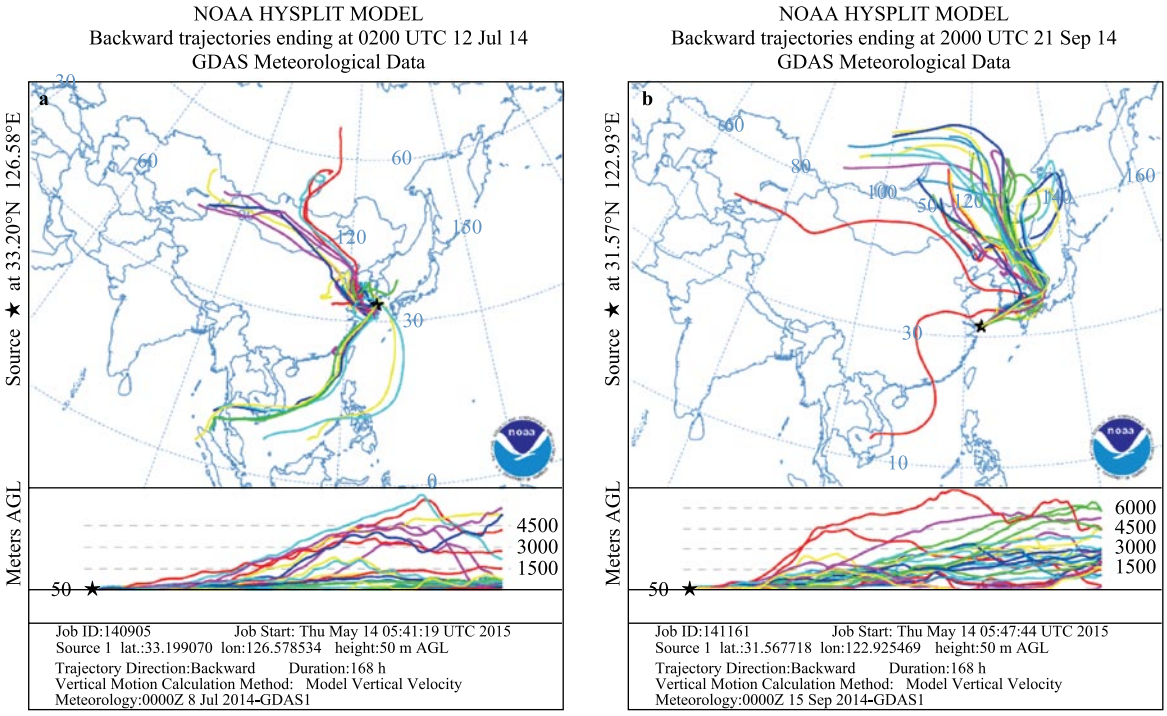

Figure 4 7-day back trajectories of the carbon monoxide maximum over the East China Sea (**a**, 12 July; **b**, 21 September).

Pacific Ocean. This represents the marine backgroud. As a result, the concentration observed at this site was close to the average over this section.

The diurnal variation of carbon monoxide concentration over different sections is shown in Figure 6. The amplitude of the variation was relatively low except for values collected over the East China Sea. The amplitude over the East China Sea reached up to 400 ppbv. This may be due to the relatively small number of samples and the intense anthropogenic emission. The amplitude over the Sea of Japan was as high as 60 ppbv. While this is higher than the other sections, it is far lower than over the East China Sea. If the data from the East China Sea is excluded, the amplitudes of the remaining sections were all lower than 20 ppbv. The amplitude over the Arctic Ocean was only 10 ppbv. The carbon monoxide concentrations in most sections reach their maximum around midnight. This may be the result of reduced sunlight which leads to a decrease in the photochemical reactions that remove carbon monoxide in the atmosphere. No double-peak was found over the pelagic seas as reported in a previous study of urban atmospheric carbon monoxide[20]. This discrepancy is probably due to a lack of anthropogenic emission. The departure and the return of R/V *XUE LONG* icebreaker were both near noontime, and the associated sampling at noon may have resulted in the maximum observation over the East China Sea.

3.2 The temporal and spatial variations of ozone

Ozone concentration measured during the 6th Chinese National Arctic Research Expedition ranged between 3.27 and 77.82 ppbv with an average of 29.47±10.48 ppbv. The time series is shown in Figure 7.

The whole course is divided into six sections according to latitudes and distaces to the coasts. The average, maximum, and minimum ozone concentration of each section is shown in Table 2.

Similar to the concentrations of carbon monoxide, the concentrations of ozone were very high over the East China Sea and the Sea of Japan (Table 2). The maximum (77.82 ppbv) of the expedition was observed on the northward course over the East China Sea. For the southward leg of the journey, the maximum (74.01 ppbv) was also observed over the East China Sea. Besides the East China Sea and the Sea of Japan,

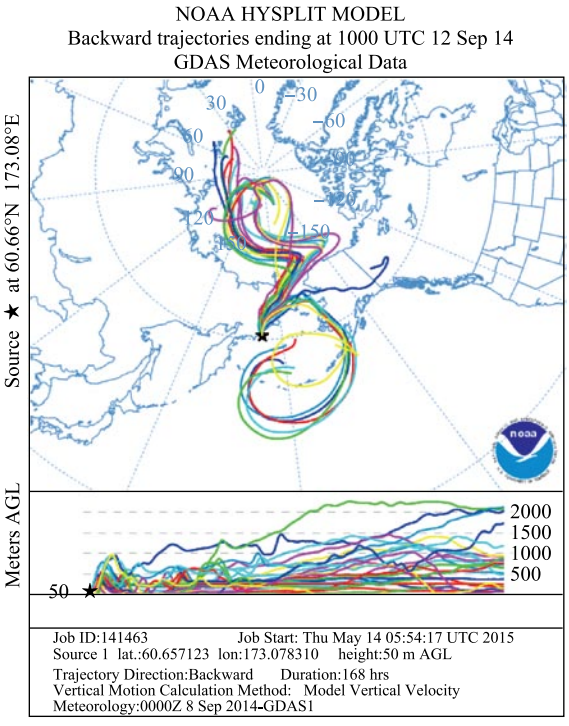

Figure 5 7-day back trajectories of the carbon monoxide maximum over the Bering Sea (12 September).

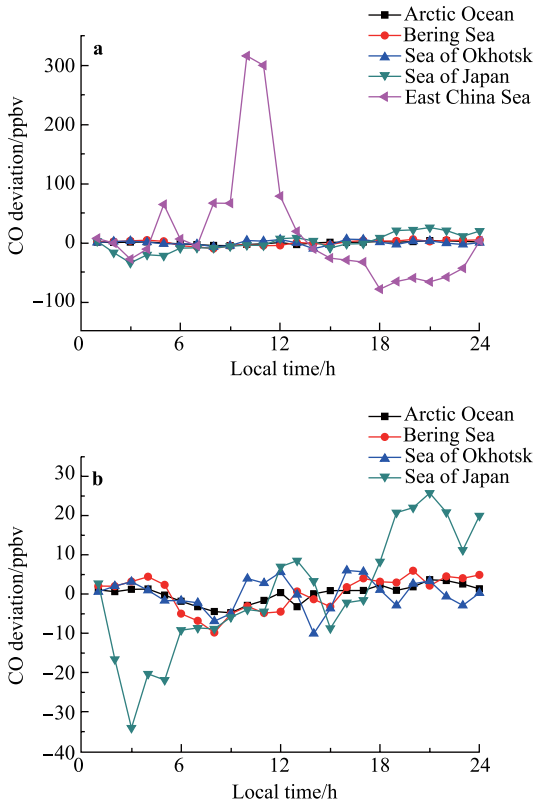

Figure 6 Diurnal variation of the concentration of carbon monoxide over different sections (**a**, East China Sea included; **b**, East China Sea excluded).

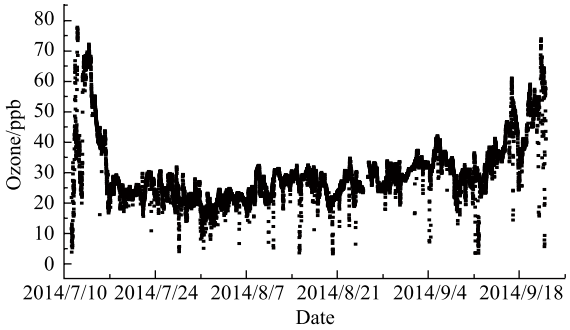

Figure 7 The time series of the concentration of ozone during the cruise.

Table 2 Ozone concentration in different sections

Sections	Date	Average/ppbv	Maximum/ppbv	Minimum/ppbv	Sample number
	7-11~7-13	37.39	77.82	3.85	260
East China Sea	9-20~9-22	53.27	74.01	5.65	140
	Overall	42.95	77.82	3.85	400
	7-13~7-15	56.59	72.24	16.17	366
Sea of Japan	9-18~9-20	48.43	59.14	37.62	324
	Overall	52.76	72.24	16.17	690
	7-15~7-19	28.21	43.68	16.71	549
Sea of Okhotsk	9-14~9-118	39.80	61.12	14.38	664
	Overall	34.56	61.12	14.38	1213
	7-19~7-28	23.92	31.90	4.00	1230
Bering Sea	9-9~9-14	28.33	38.56	3.43	582
	Overall	25.32	38.56	3.43	1756
Arctic Ocean	7-28~9-9	26.10	42.15	3.27	5988
Overall	7-11~9-22	29.47	77.82	3.27	10047

observed ozone concentrations in the other sections, such as the Sea of Okhotsk, the Bering Sea, and the Arctic Ocean, were relatively low. The minimum (3.27 ppbv) was observed over the Arctic Ocean.

The concentration of ozone in the atmosphere is not directly affected by human activities, but it is affected by the carbon monoxide, precursors of ozone (e.g. nitrogen oxides), sunlight, and the oxidative ability of the atmosphere. However, the relatively high concentrations of ozone observed over the East China Sea and the Sea of Japan could still indicate the impact of intensive human activity on the concentration of ozone. The 7-day back trajectories imply that the high values were affected by continental air masses (Figure 4). There is an evident decrease in the ozone concentration with increasing latitude over the mid-latitude seas. When the R/V *XUE LONG* icebreaker entered high-latitude seas, there was a reduction in the rate of decrease (Figure 8).

The diurnal variation of ozone concentration over different sections is shown in Figure 9. Similar to carbon monoxide, the amplitude of the variation was relatively low except for values over the East China Sea. The amplitude over the East China Sea reached up to 60 ppbv, which may be due to the relatively small number of samples and intensive anthropogenic emission. If the data from the East China Sea is excluded, the amplitudes of the other sections were all lower than 10 ppbv. The amplitude was only 5 ppbv over the Arctic Ocean. The ozone concentration in most sections started to decrease immediately after the sunrise and reaching their minimum around noon. The daytime ozone losses in the marine boundary layer over these sections maybe due to not only the photochemistry involving NO_X cycles but also by the sunrise ozone destruction which seems to be caused by the halogen species, such as Br. The halogen species in the marine boundary layer may be released from sea-salt particles reacting with pollutants. If the Br_2 released from

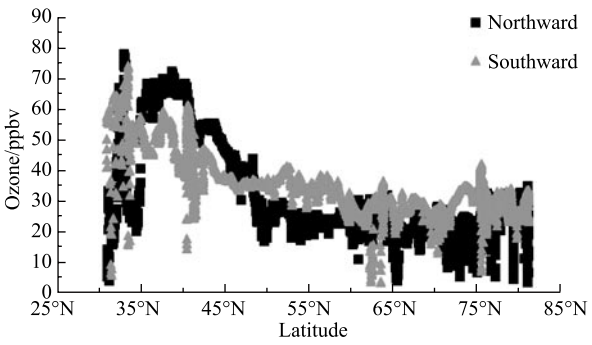

Figure 8 The concentration of ozone at different latitudes.

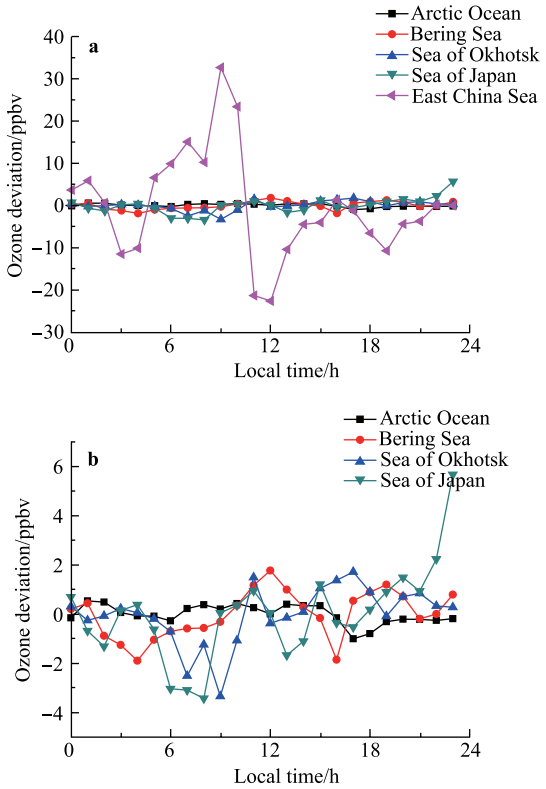

Figure 9 Diurnal variation of the concentration of ozone over different sections (**a**, East China Sea included; **b**, East China Sea excluded).

sea-salts is accumulated in the marine boundary layer in the nighttime, Br radical which destructs ozone catalytically is easily formed by the feeble solar radiation just after sunrise[12]. The observed maximum over the East China Sea was at noon because that was the time the R/V *XUE LONG* icebreaker departed from and returned to the harbor with its high levels of anthropogenic emission.

3.3 The correlation between carbon monoxide and ozone

The analysis of the relationship between carbon monoxide and ozone could provide information about the source of the air masses[21-22]. Figure 10 shows the correlation between carbon monoxide and ozone.

In most sections, such as the East China Sea, the Sea of Japan, the Sea of Okhotsk, and the Arctic Ocean, there were positive correlations between carbon monoxide and ozone (r = 0.34−0.60). This indicates that the ozone observed during the expedition likely originated from photochemical reactions of carbon monoxide[23-24]. The regression slopes for the East China Sea and the Sea of Japan are relatively lower than those of the Sea of Okhotsk and the Arctic Ocean due to the anthropogenic emissions in Northeastern Asia[25].

However, the positive correlation was weak (r = 0.09) in the Bering Sea section. This suggests an air mass source quite distant from the surface CO emission sources. In addition, the tropopause heights are relatively low in the high latitude regions. This indicates a possible downward transport of the lowermost stratospheric ozone into the troposphere[26].

4 Conclusion

The concentrations of carbon monoxide and ozone in the

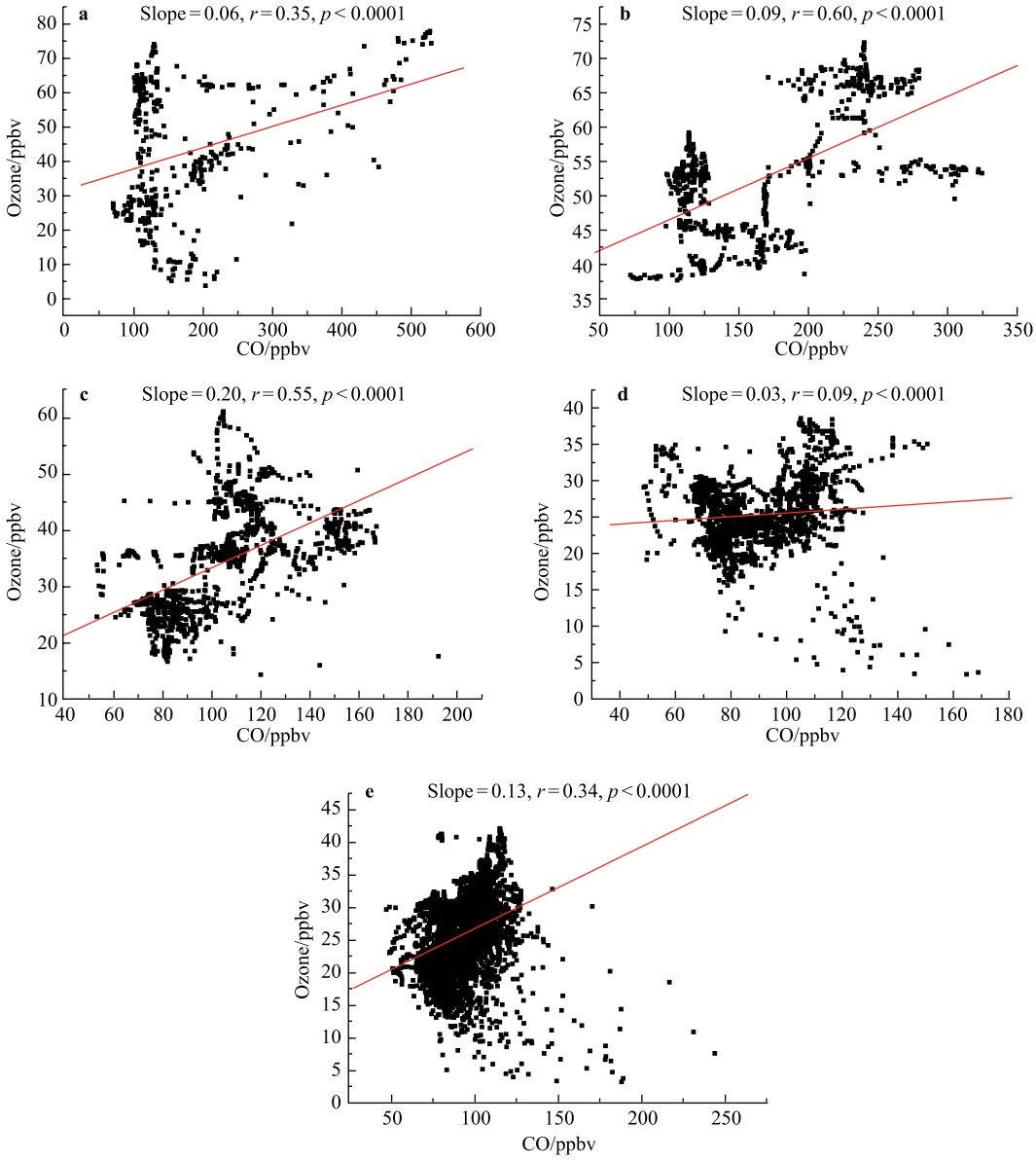

Figure 10 Correlation between ozone and carbon monoxide in each section (**a**, East China Sea; **b**, Sea of Japan; **c**, Sea of Japan; **d**, Bering Sea; **e**, Arctic Ocean).

marine boundary layer were measured aboard the R/V *XUE LONG* icebreaker using internet-enabled analyzers. Samples were taken during the 6th Chinese National Arctic Research Expedition from July to September 2014.

Carbon monoxide concentration measured during the journey ranged between 47.00 and 528.52 ppbv with an average of 103.59 ± 40.37 ppbv. The concentrations over mid-latitude and coastal seas were much higher than over high-latitude and pelagic seas, probably owing to anthropogenic emission. The maximum was observed over the East China Sea, and almost all the extremely high values were observed over coastal seas. The concentration over pelagic seas was much lower than over the East China Sea and the Sea of Japan, and the amplitudes of the diurnal variations were also smaller. Ozone concentration measured during the cruise ranged between 3.27 and 77.82 ppbv with an average of 29.46 ± 10.48 ppbv. There was a gradient of ozone concentration outside the Arctic Ocean which decreased sharply with the increasing latitude (during both the northward and the southward courses). However, no significant variation was observed over the Arctic Ocean. Similar to carbon monoxide, the diurnal variation over high-latitude seas and the Arctic Ocean was very small. The positive correlation between carbon monoxide and ozone in most sections suggests that the ozone in the marine boundary layer mainly originated from photochemical reactions involving carbon monoxide. However, the weak correlation over the Bering Sea may be affected by the input of stratospheric ozone.

Acknowledgments This work was supported by the Chinese Polar Environment Comprehensive Investigation & Assessment Programs (Grant no. CHINARE 2011-2015), the National Natural Science Foundation of China (Grant no. 41176170). We thank the NOAA Air Resources Laboratory (ARL) for making the HYSPLIT transport and dispersion model available on the Internet (http://www.arl.noaa.gov/ready.html).

References

1 Daniel J S, Solomon S. On the climate forcing of carbon monoxide. J Geophys Res, 1998, 103(D11): 13249–13260
2 Seiler W, Junge C. Carbon monoxide in the atmosphere. J Geophys Res, 1970, 75(12): 2217–2226
3 Seiler W. The cycle of atmospheric CO. Tellus, 1974, 26(1-2): 116–135
4 Müller J F, Stavrakou T. Inversion of CO and NO_x emissions using the adjoint of the IMAGES model. Atmos Chem Phys, 2005, 5(5): 1157–1186
5 Thompson A M. The oxidizing capacity of the Earth's atmosphere: Probable past and future changes. Science, 1992, 256(5060): 1157–1165
6 Kanakidou M, Crutzen P J. The photochemical source of carbon monoxide: Importance, uncertainties and feedbacks. Chemos Global Change Sci, 1999, 1(1-3): 91–109
7 Novelli P C, Masarie K A, Lang P M. Distributions and recent changes of carbon monoxide in the lower troposphere. J Geophys Res, 1998, 103(D15): 19015–19033
8 Holloway T, Levy H I I, Kasibhatla P, et al. Global distribution of carbon monoxide. J Geophys Res, 2000, 105(D10): 12123–12147
9 Bian L G, Tang J, Lai X, et al. Monitoring carbon monoxide during 2008–2010 at Zhongshan Station, Antarctica. Acta Sci Circum, 2014, 34(2): 310–317 (in Chinese)
10 Yurganov L N, Grechko E I, Dzhola A V. Carbon monoxide and total ozone in Arctic and Antarctic regions: seasonal variations, long-term trends and relationships. Sci Total Environ, 1995, 160–161: 831–840
11 Yurganov L N. Seasonal cycles of carbon monoxide over the Arctic and Antarctic: total columns versus surface data. Atmos Res, 1997, 44(1–2): 223–230
12 Watanabe K, Nojiri Y, Kariya S. Measurements of ozone concentrations on a commercial vessel in the marine boundary layer over the northern North Pacific Ocean. J Geophys Res Atmos, 2005, 110(D11): D11310
13 Wang Y T, Bian L G, Ma Y F, et al. Surface ozone monitoring and background characteristics at Zhongshan Station over Antarctica. Chin Sci Bull, 2011, 56(10): 1011–1019
14 Bojkov R D, Fioletov V E. Estimating the global ozone characteristics during the last 30 years. J Geophys Res, 1995, 100(D8): 16537–16551
15 Johnson J E, Gammon R H, Larsen J, et al. Ozone in the marine boundary layer over the Pacific and Indian Oceans: Latitudinal gradients and diurnal cycles. J Geophys Res Atmos, 1990, 95(D8): 11847–11856
16 Park K, Rhee T S. Source characterization of carbon monoxide and ozone over the Northwestern Pacific in summer 2012. Atmos Environ, 2015, 111: 151–160
17 Zhang J K, Liu W, Han Y Y, et al. Progresses in influence of variations in stratospheric ozone on tropospheric climate. J Arid Meteor, 2014, 32(5): 685–693 (in Chinese)
18 Draxler R R. Evaluation of an ensemble dispersion calculation. J Appl Meteor, 2003, 42(2): 308–317
19 Draxler R R, Hess G D. An overview of the HYSPLIT 4 modelling system for trajectories, dispersion, and deposition. Aust Meteor Mag, 1998, 47: 295–308
20 Huang X, Huang X X, Wang T J, et al. Observation and analysis of urban upper atmospheric carbon monoxide in Nanjing. China Environ Sci, 2013,33(9): 1577–1584 (in Chinese)
21 Parrish D D, Holloway J S, Trainer M, et al. Export of North American ozone pollution to the north Atlantic Ocean. Science, 1993, 259(5100): 1436–1439
22 Harris J M, Dlugokencky E J, Oltmans S J, et al. An interpretation of trace gas correlations during Barrow, Alaska, winter dark periods, 1986–1997. J Geophys Res, 2000, 105(D13): 17267–17278
23 Chin M, Jacob D J, Munger J W, et al. Relationship of ozone and carbon monoxide over North America. J Geophys Res, 1994, 99(D7): 14565–14573
24 Parrish D D, Trainer M, Holloway J S, et al. Relationships between ozone and carbon monoxide at surface sites in the North Atlantic region. J Geophys Res, 1998, 103(D11): 13357–13376
25 Ding A J, Wang T, Xue L K, et al. Transport of north China air pollution by mid latitude cyclones: Case study of aircraft measurements in summer 2007. J Geophys Res, 2009, 114(D8): D08304
26 Lee S, Feldstein S B. Detecting ozone- and greenhouse gas–driven wind trends with observational data. Science, 2013, 339(6119): 563–567